Smart Drug-Loaded Polymer Gold Nanoshells for Systemic and Localized Therapy of Human Epithelial Cancer

ARTICLE *in* ADVANCED MATERIALS · NOVEMBER 2009

Impact Factor: 17.49 · DOI: 10.1002/adma.200900334

Smart Drug-Loaded Polymer Gold Nanoshells for Systemic and Localized Therapy of Human Epithelial Cancer

By *Jaemoon Yang, Jaewon Lee, Jinyoung Kang, Seung Jae Oh, Hyun-Ju Ko, Joo-Hiuk Son, Kwangyeol Lee, Jin-Suck Suh, Yong-Min Huh,** and *Seungjoo Haam**

The remarkable physicochemical properties of nanomaterials have allowed nanoplatform-based integration medical strategies for combinatorial cancer treatments concomitant with real-time diagnosis.[1] In particular, novel photothermal effects of gold nanostructures and carbon nanotubes activated by near-infrared (NIR) light irradiation are being actively studied for their tumoricidal efficacies.[2] While these nanomaterials can certainly increase the local temperature around cancerous regions by NIR light, it is not entirely evident that the photothermal effect is sufficient to achieve the desired level of cancer-cell cytotoxicity with a wide range.[1b,3] Furthermore, the short penetration depth of the NIR laser might require a rather invasive optical-fiber-containing needle and/or endoscope insertion into the tumor tissue in order to access and treat deep-seated cancer cells by hyperthermia. Deep treatment is unavoidable to eliminate the source of marginal recurrence, and the local heat generated by the nanomaterials would undoubtedly generate searing pain to the patients.[4] Thus, for patient compliance, the development of methods for greatly enhancing the tumoricidal efficacy of nanoplatform-based cancer treatment by combination of systemic chemotherapy is vital. Because chemical drugs encapsulated in nanoplatforms can diffused into a wide range of cancerous parts and induce apoptosis of target cancer cells.[1a]

Herein, we report a novel nanotherapeutic system consisting of a poly(lactic-*co*-glycolic acid) (PLGA) matrix containing doxorubicin (DOX) as a chemotherapeutic agent and a gold over-layer on a polymer matrix capable of a photothermal effect. For targeted delivery to human epithelial cancer cells, anti-EGFR (epithermal growth factor receptor) antibody (Cetuximab) was conjugated on the gold nanoshell surface (Fig. 1). This nanoplatform is capable of efficient antibody-mediated binding and internalization against EGFR-overexpressed cancer cells, resulting in an antibody-induced tumoricidal effect by blocking the EGFR pathway.[2b] Furthermore, the temperature increase due to the surface plasmon resonance (SPR) effect of the gold-layer leads to potential photothermal tumoricidal effect,

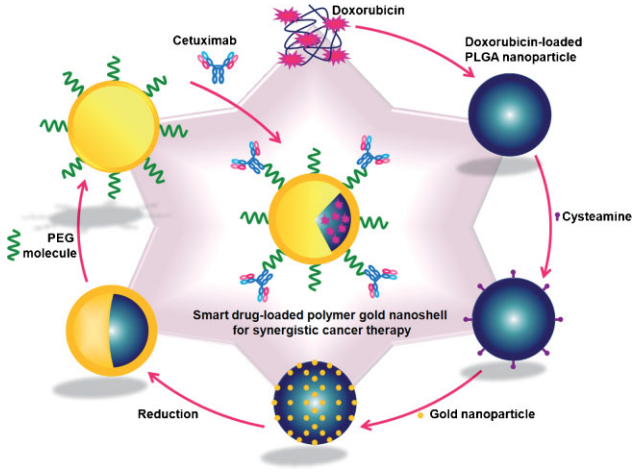

Figure 1. Schematic illustration of multifunctional drug-loaded gold nanoshells for synergistic cancer therapy. The novel nanostructure comprises three key parts for multidimensional therapeutic potentials, namely, I) an anti-EGFR antibody, Cetuximab (CET), as a targeting moiety and signal-transduction inhibitor, II) a gold nanoshell that has a photothermal effect due to plasmon resonance upon illumination by an NIR laser, and III) DOX as a chemotherapeutic agent. These three components, incorporated into PLGA nanoparticles, provide synergistic tumoricidal efficacy.

[*] Prof. Y.-M. Huh, Dr. J. Yang, Dr. S. J. Oh, H.-J. Ko, Prof. J.-S. Suh
Department of Radiology
Yonsei University
Seoul, 120-752 (Republic of Korea)
E-mail: ymhuh@yuhs.ac
Prof. S. Haam, Dr. J. Yang, J. Lee, J. Kang
Department of Chemical and Biomolecular Engineering
Yonsei University
Seoul, 120-749 (Republic of Korea)
E-mail: haam@yonsei.ac.kr
Dr. S. J. Oh
Brain Korea 21 Project for Medical Science
Yonsei University
Seoul, 120-749 (Republic of Korea)
Prof. J.-H. Son
Department of Physics
University of Seoul
Seoul, 130-743 (Republic of Korea)
Prof. K. Lee
Department of Chemistry, Korea University
Seoul 136-701 (Republic of Korea)

DOI: 10.1002/adma.200900334

while facilitating the release of DOX from the softened PLGA matrix at temperatures over its glass-transition temperature to reinforce the cytotoxic effect of the nanoplatform.[5]

DOX-loaded PLGA nanoparticles (DPNP) ((80 ± 10) nm) were formed by a nanoemulsion method.[1a,6] Subsequently, gold nanoshells on DPNP (DPGNS, DOX-loaded PLGA gold nanoshells) were prepared by fixation of gold nanoparticles (GNP) on the surface of DPNP as seeds followed by formation of a gold nanolayer onto the existing gold nanoparticles to induce a photothermal effect by NIR laser irradiation (Fig. 1).[2b] The carboxyl group of DPNP was reacted with cysteine via a carbodiimide-mediated conjugation process to display the sulfhydryl group at the outer extremity, which fixed GNPs onto the surface of DPNP.[2b] Subsequently, a gold nanolayer was formed on the surface of DPNP by reduction of tetrachloroaurate (III) trihydrate (Fig. S1 of the Supporting Information (SI)). The morphology of DPGNS was confirmed by transmission electron microscopy (TEM, Fig. 2a). X-ray photoelectron spectroscopic measurements of DPNPs exhibited an O 1s orbital peak (290 eV) and a C 1s orbital peak (537 eV) due to the polymeric components, and an Au 1s orbital peak (88 eV) due to the Au component (Fig. S2 of SI). Moreover, the surface plasmon peak of GNP at 520 nm was shifted to the red-color region after the formation of a gold nanolayer, with GNP-attached DPNP at 548 nm and DPGNS at 775 nm (Fig. 2b). The detection of Au and its strong SPR feature is consistent with a gold nanoshell formed around the dielectric core of the DPNP. Furthermore, the plasmon peak was not distorted nor broadened during the formation of the gold nanolayer.[7] These results demonstrated that a reticular structure of the gold nanolayer was successfully generated on the surface of DPNP. This structure enables for an effective thermal induced tumoricidal system using SPR because of minimal absorption by water and hemoglobin at the NIR region, in contrast to a complete, void-less gold shell.[2e] This reticular structure of DPGNS, in turn, conveniently enables DOX release through the porous gold layer.

To investigate the hyperthermic potential of DPGNS, the heat generated by NIR laser irradiation (820 nm and 15 W cm^{-2} for 10 min) was measured and visualized (Fig. 2c). The temperature of the DPGNS solution increased by 14.3 °C compared to pure water without DPGNS. This temperature elevation of the DPGNS solution was also affirmed by thermal images recorded using an IR camera that showed a deep red color (DPGNS) versus a blue color (pure water, Fig. 2c, insets). The thermal effect of DPGNS with NIR laser demonstrated latent capability for ablation of cancer cells. The heat generated by DPGNS under NIR irradiation, furthermore, is sufficiently higher than the glass-transition temperature of PLGA (45 °C) to induce a sudden drug release of DOX from DPGNS; the amount of DOX released from DPGNS was steeply increased (Fig. 2d), coincident with NIR laser irradiation (820 nm and 15 W cm^{-2} for 10 min). The additional 14 μg of DOX release is certainly useful for increasing the tumoricidal effects of the nanoplatform.

Because targeted delivery to specific cells is essential to systemic cancer therapy, an anti-EGFR antibody, Cetuximab-conjugated DPGNS (CET-DPGNS), was attached to the nanoplatform by a bioconjugation technique (Method in SI), and the cellular targeting efficacy was investigated for two different cancer cell lines, EGFR-abundant A431 cells and EGFR-deficient MCF7 cells.[2b] An irrelevant antibody, human IgG-conjugated DPGNS (IgG-DPGNS), was also prepared as a control for the experiment. Flow-cytometry analysis showed the specific binding efficiency of CET-DPGNS (Fig. S3 of SI and Fig. 3a). A431 cells treated with CET-DPGNS exhibited six times higher fluorescence intensity (ΔFI/FI$_{non\text{-}treated}$; FI: fluorescence intensity) than MCF7 cells, in accordance with the difference in expression level of receptors. The relative

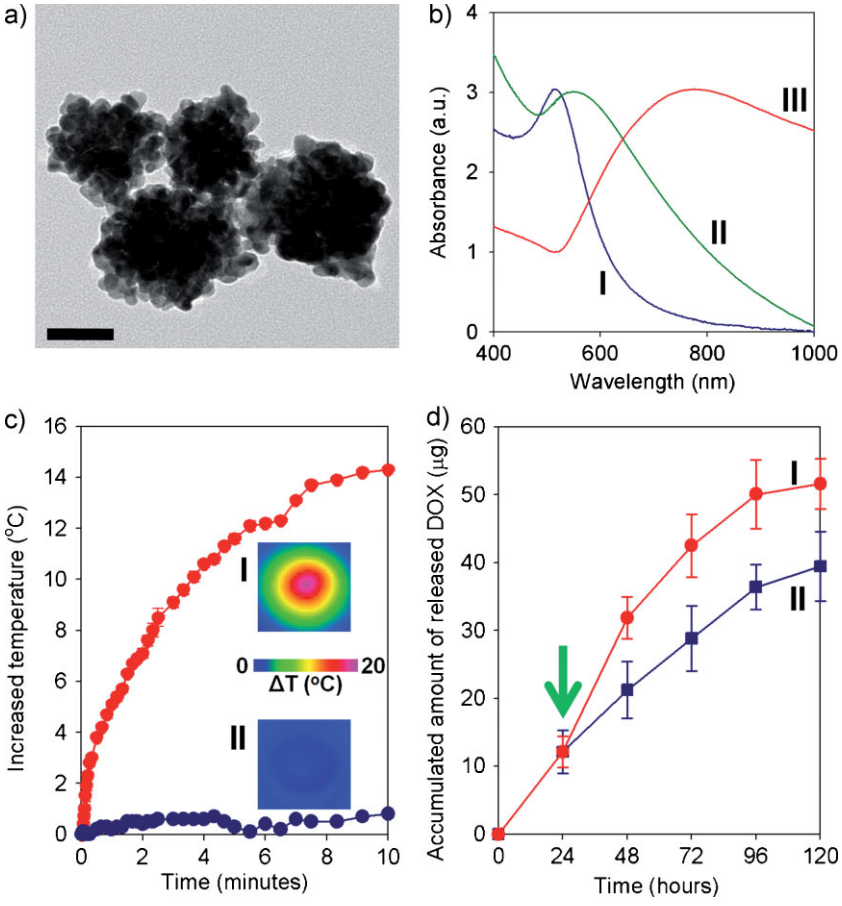

Figure 2. a) TEM images of DPGNS. Scale bar: 50 nm. b) UV-vis absorption bands of I) DPGNS, II) GNP-coated DPNP, and III) DPGNS. c) Increased temperature versus irradiation time due to plasmon resonance of DPGNS after NIR laser irradiation (820 nm and 15 W cm^{-2} for 10 min); I) DPGNS solution (13 mg mL^{-1}) and II) pure water. Inset: thermal images recorded by infrared camera of DPGNS solution (upper) and pure water (lower). d) DOX release patterns of I) DPGNS and II) DPGNS irradiated by NIR laser (green arrow indicates onset of NIR irradiation with 820 nm and 15 W cm^{-2} for 10 min) for 120 h, respectively.

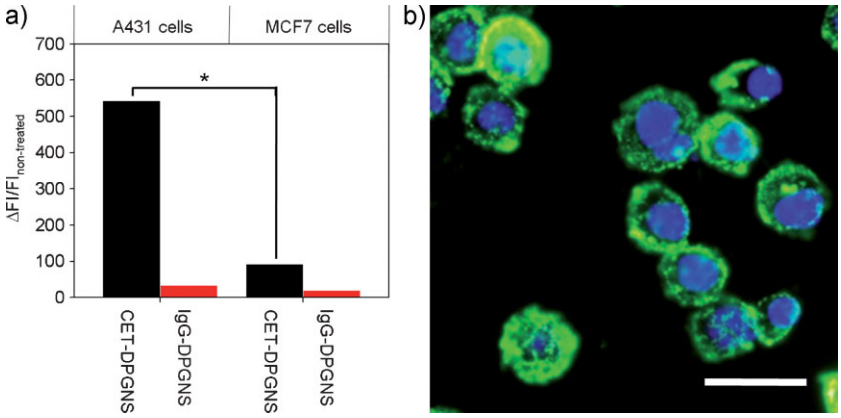

Figure 3. a) Relative fluorescence intensities ($\Delta FI/FI_{non\text{-}treated}$; FI: fluorescence intensity) using flow cytometry analysis ($^*p < 0.05$). b) Fluorescence microscopic images of A431 cells treated with CET-DPGNS. The bright green-light emission from binding of fluorescein isothiocyanate-labeled goat anti-CET antibody indicates successful binding of CET-DPGNS to target cells, and the blue indicates cell nuclei. Scale bar: 20 μm.

fluorescence intensity of IgG-DPGNS was insignificant because of its non-specificity against cancer cells. In fluorescence microscopic imaging, A431 cells treated with CET-DPGNS showed a bright green color, due to the fluorescein isothiocyanate of the secondary antibody and the blue color indicating nuclear-site stained by 4′,6-diamidino-2-phenylindole (Fig. 3b). Furthermore, binding efficiency of CET-DPGNS to A431 cells was 64%, evaluated by measuring of Au component via inductively coupled plasma atomic-emission spectrometry (ICP-AES). These results demonstrate that CET-DPGNS exhibits a remarkable cellular affinity for EGFR-abundant cell lines.

To evaluate the localized tumoricidal potential of our polymer gold nanoshells, A431 and MCF7 cells were treated with CET-PGNS, IgG-PGNS, CET-DPGNS, or IgG-DPGNS, respectively. As a previous mention, CET-DPGNS can specifically bind to EGFR-abundant A431 cells and generate a hyperthermic effect from gold nanoshells by illumination with an NIR laser (820 nm and 15 W cm^{-2} for 10 min). At higher temperatures, intracellular proteins are denatured, inhibiting normal cellular growth and proliferation.[8] For qualitative analysis, we used viable fluorescent cell staining with calcein AM. In fluorescence microscopic images (Fig. 4a), a dark hole from thermal-induced tumoricidal efficacy was observed only for A431 cells treated with CET-PGNS or CET-DPGNS. In contrast, a vivid green color was observed for the other samples, indicating weak localized nanostructure-induced cytotoxic effects. These microscopic images demonstrate that CET-PGNS and CET-DPGNS with a gold layer are successfully localized-photothermal agents with NIR laser irradiation.

We further evaluated the multidimensional therapeutic potential of multifunctional polymer gold nanoshells based on systemic chemotherapy (CET and DOX) together with localized hyperthermia from gold nanolayer and NIR laser. The cell viabilities (CV) of A431 cells treated with CET-PGNS or CET-DPGNS in the absence of laser illumination were $(91.5 \pm 4.9)\%$ ($CV_{CET\text{-}PGNS}$) and $(86.7 \pm 5.3)\%$ ($CV_{CET\text{-}DPGNS}$), respectively, as measured by 3-(4,5-Dimethylthiazol-2-yl)-2,5-diphenyltetrazolium bromide (MTT) assays. These similar cell viabilities indicate that the amount of DOX released from CET-DPGNS was too low to inhibit tumor-cell proliferation within 24 h. After laser illumination, however, laser-induced hyperthermic tumoricidal effects for A431 cells treated with CET-PGNS or CET-DPGNS were 55.1% $((CV_{CET\text{-}PGNS} - CV_{CET\text{-}PGNS+laser})/CV_{CET\text{-}PGNS})$ and 69.8% $((CV_{CET\text{-}DPGNS} - CV_{CET\text{-}DPGNS+laser})/CV_{CET\text{-}DPGNS})$, respectively. Notably, CET-DPGNS exhibited an additional cytotoxic effect of 36.2% $((CV_{CET\text{-}PGNS+laser} - CV_{CET\text{-}DPGNS+laser})/CV_{CET\text{-}PGNS+laser})$ compared with CET-PGNS due to the remote-controlled burst-release of DOX from DPGNS. The photothermal effect of the gold nanolayer partially melted the core polymeric substrate, releasing a large amount of DOX from DPGNS for additional cytotoxic activity against the target cancer-cell line. In contrast, IgG-DPGNS demonstrated a minimal cytotoxic effect for both A431 and MCF7 cells due to the absence of an EGFR-specific targeting route.

After 48 h of further incubation, the cell viabilities of both cell types treated with each nanostructure were closely examined to reveal additional systemic cytotoxicity by the chemotherapeutic agents (Fig. 4c). The cell viability of A431 cells treated with the nanostructures was drastically decreased due to the growth inhibitory effects from CET and DOX (Fig. S4 of SI). In the case of CET-DPGNS, the cell viability was $(15.4 \pm 4.3)\%$ and this nanoplatform exhibited the greatly enhanced cytotoxic effect of 41.2% $((CV_{24H} - CV_{72H}/CV_{24H}$, $^*p < 0.05)$. In particular, remote-controlled burst-release of drugs exhibited a synergistic therapeutic efficacy of 41.1% $((CV_{CET\text{-}PGNS+laser} - CV_{CET\text{-}DPGNS+laser})/CV_{CET\text{-}PGNS+laser}$ at 72 h, $^{**}p < 0.05)$, which was four times larger than the same treatment without NIR laser illumination (11.9%; $(CV_{CET\text{-}PGNS} - CV_{CET\text{-}DPGNS})/CV_{CET\text{-}PGNS}$ at 72 h). These results demonstrate the excellent target-specificity and gold-nanoshell-driven hyperthermic efficacies of CET-DPGNS. Moreover, systemic cytotoxicity of CET and released DOX can compensate for localized cytotoxicity by photothermal effect alone.

In conclusion, we fabricated multifunctional smart polymer gold nanoshells (CET-DPGNS), composed of chemotherapeutic agents (therapeutic antibody and anticancer drug-loaded polymeric nanoparticles) for systemic chemotherapy, and a polymer-based gold nanoshell for localized photothermal treatment by NIR laser illumination. We believe that our tailored nanoplatform, which employs a combination of systemic and localized cancer therapies and is capable of producing cumulative cytotoxicity in tumors due to i) the tumoristatic effect of the therapeutic antibody, ii) controlled 'burst release' of drugs by extra NIR light, and iii) potential hyperthermia of the gold nanoshell. In the early future, furthermore, an in vivo study using our multifunctional nanoplatforms may remarkably improve the methodologies for effective cancer therapy.

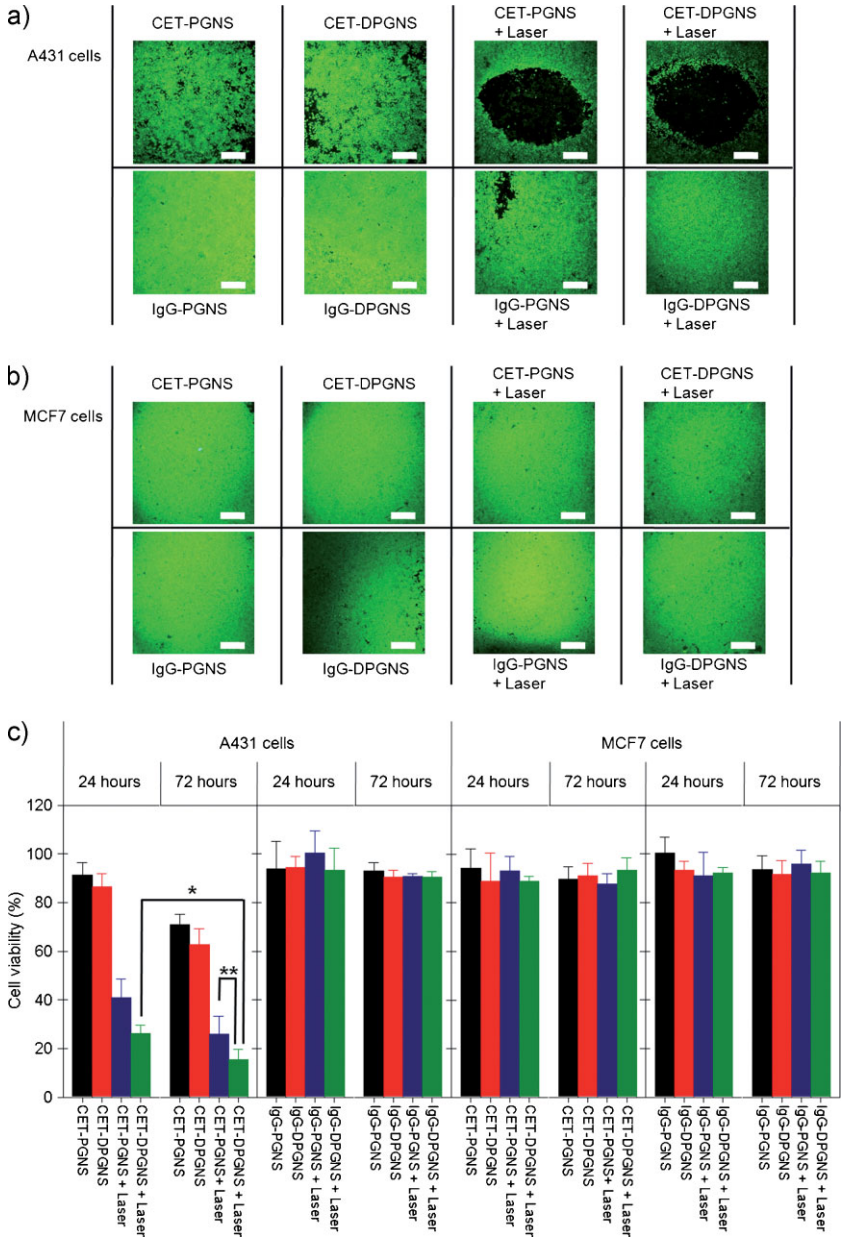

Figure 4. Therapeutic efficacies of multifunctional smart polymer gold nanoshells: fluorescence images of a) A431 and b) MCF7 cells treated with CET-PGNS, CET-DPGNS, IgG-PGNS, and IgG-DPGNS, respectively. After NIR laser exposure (820 nm and 15 W cm^{-2} for 10 min), the cells were further incubated for 48 h. All scale bars: 250 μm. c) Cell viability of CET-PGNS, CET-DPGNS, IgG-PGNS, and IgG-DPGNS for A431 and MCF7 cells (* and ** both, $p < 0.05$).

Acknowledgements

J. Y and J. L. contributed equally to this work. This work was supported by the Korea Science and Engineering Foundation grant funded by the Korea government (M10755020001-07N5502-00110, R15-2004-024-00000-0, 2007-04717) and the Korea Health 21 R&D Project, Ministry of Health &Welfare (A085136), Yonsei University College of Medicine (6-2008-0223), Republic of Korea. Supporting Information is available online from Wiley InterScience or from the author.

Received: January 30, 2009
Revised: April 17, 2009
Published online:

[1] a) J. Yang, C.-H. Lee, H.-J. Ko, J.-S. Suh, H.-G. Yoon, K. Lee, Y.-M. Huh, S. Haam, *Angew. Chem. Int. Ed.* **2007**, *46*, 8836. b) X. Huang, I. H. El-Sayed, W. Qian, M. A. El-Sayed, *J. Am. Chem. Soc.* **2006**, *128*, 2115.

[2] a) A. Joshi, S. Punyani, S. S. Bale, H. Yang, T. Borca-Tasciuc, R. S. Kane, *Nat. Nanotechnol.* **2008**, *3*, 41. b) J. Lee, J. Yang, H. Ko, S. J. Oh, J. Kang, J.-H. Son, K. Lee, S.-W. Lee, H.-G. Yoon, J.-S. Suh, Y.-M. Huh, S. Haam, *Adv. Funct. Mater.* **2008**, *18*, 258. c) B. Radt, T. A. Smith, F. Caruso, *Adv. Mater.* **2004**, *16*, 2184. d) S. K. Ghosh, T. Pal, *Chem. Rev.* **2007**, *107*, 4797. e) J. Chen, D. Wang, J. Xi, L. Au, A. Siekkinen, A. Warsen, Z. Y. Li, H. Zhang, Y. Xia, X. Li, *Nano Lett.* **2007**, *7*, 1318.

[3] L. R. Hirsch, R. J. Stafford, J. A. Bankson, S. R. Sershen, B. Rivera, R. E. Price, J. D. Hazle, N. J. Halas, J. L. West, *Proc. Natl. Acad. Sci. USA* **2003**, *100*, 13549.

[4] http://www.laserpartner.cz/lasp/web/en/2000/0015.htm (Accessed on May 25, 2009).

[5] a) B. S. Zolnik, P. E. Leary, D. J. Burgess, *J. Controlled Release* **2006**, *112*, 293. b) N. Faisant, J. Akiki, F. Siepmann, J. P. Benoit, J. Siepmann, *Int. J. Pharm.* **2006**, *314*, 189. c) H. Park, J. Yang, S. Seo, K. Kim, J. Suh, D. Kim, S. Haam, K.-H. Yoo, *Small* **2008**, *4*, 192.

[6] J. Yang, C.-H. Lee, J. Park, S. Seo, E.-K. Lim, Y. J. Song, J.-S. Suh, H.-G. Yoon, Y.-M. Huh, S. Haam, *J. Mater. Chem.* **2007**, *17*, 2695.

[7] V. Salgueirino-Maceira, M. A. Correa-Duarte, M. Farle, A. Lopez-Quintela, K. Sieradzki, R. Diaz, *Chem. Mater.* **2006**, *18*, 2701.

[8] D. Hanahan, R. A. Weinberg, *Cell* **2000**, *100*, 57.